

# Optical generation of 16-tupling millimeter-wave signal without optical filtering

XIAOGANG CHEN<sup>a,\*</sup>, LU XIA<sup>a</sup>, DEXIU HUANG<sup>b</sup>

<sup>a</sup>*School of Electrical and Photoelectronic Engineering, Changzhou Institute of Technology, Changzhou, Jiangsu, 213032 China*

<sup>b</sup>*Wuhan National Laboratory for Optoelectronics (WNLO), Huazhong University of Sci & Tech, Wuhan, Hubei, 430074 China*

A novel scheme is proposed for frequency 16-tupling millimeter-wave generation based on two cascaded integrated dual-parallel Mach-Zehnder modulators (MZM) without optical filtering. The impact of imperfect extinction ratio (EXT) of MZM on system performance is investigated. The improvement of system performance through MZM modulation index optimization is also analyzed. Simulation verifications are provided for the microwave frequency multiplication scheme. In addition, the impact of MZM bias drift and phase drift on optical mm-wave generation is analyzed.

(Received July 19, 2017; accepted August 9, 2018)

**Keywords:** Microwave Photonics, 16-tupling, Mach-Zehnder modulators, Extinction ratio, Modulation index optimization

## 1. Introduction

With the accelerated development of broadband wireless communication, phase array antenna, millimeter-wave imaging, and radar, efficient and cost-effective methods of generation and transmission microwave/millimeter-wave signals are of utmost importance [1, 2]. In addition, mm-wave signal generations with frequency beyond 60 GHz are essential for various applications with the increasing of intended mm-wave frequency.

To transmit mm-wave signals over a long distance, optical mm-wave signal [3] based on low transmission loss optical fiber network is a cost-effective and viable solution. Various techniques have been proposed to generate high-frequency electrical signals in the optical domain. Among these techniques, optical mm-wave generation using LiNbO<sub>3</sub> Mach-Zehnder modulator (MZM) are the most reliable approach [4-8]. Nevertheless, the generation of high frequency optical mm-wave signals is limited by the frequency response of MZM, which is typically less than 40 GHz. Moreover, radio-frequency (RF) components with frequency response over 26 GHz are considerably more expensive than those below 26 GHz. Additionally, the optical filtering hinders the implementation of optical up-conversion in wavelength division multiplexing (WDM) radio over fiber (RoF) systems. Therefore, the frequency multiplication technique without optical filters is of great interest. Several frequency 16-tupling optical mm-wave generation schemes are presented [9, 10], the impact of non-ideal extinction ratio (EXT) of MZM on system performance is

not investigated thoroughly or accurate controlling of phase shift between the cascaded MZMs is required to suppress undesired optical harmonics.

In this paper a novel scheme is proposed to generate the optical mm-wave with 16-fold frequency of the local oscillator using two cascaded integrated dual-parallel MZMs (DP-MZM) [11,12]. 64 GHz mm-wave has been obtained from 4 GHz microwave signal, which reduces the frequency requirement of the modulator and the oscillator greatly. Optical mm-wave signals with frequency up to 320 GHz can be achieved by the proposed 16-tupling scheme if two 20 GHz DP-MZMs are employed.

## 2. Principle

### 2.1. Frequency 16-tupling mm-wave Generation

The principle diagram of 16-tupling optical mm-wave generation using two cascaded DP-MZMs is shown in Fig. 1. The lightwave  $E_0 e^{j\omega_0 t}$  emitted from the laser diode (LD) is injected into the first DP-MZM, which consists of two sub-MZMs (MZM1-a and MZM1-b) in parallel. Both of the sub-MZMs are biased at the full point. A  $\pi/2$  phase shift is introduced between the RF driven signals of MZM1-a and MZM1-b, and the RF driven signal applied to MZM1-a and MZM1-b can be expressed as  $V_{1a}(t) = V_m \sin \omega_m t$  and  $V_{1b}(t) = V_m \sin(\omega_m t + \pi/2)$ , respectively. Therefore, the optical field at the output of the first DP-MZM can be expressed as:

$$\begin{aligned}
E_1(t) &= \frac{1}{4} E_0 e^{j\omega_c t} \left\{ \left[ e^{\frac{j\pi V_m \sin \omega_m t}{V_\pi}} + e^{-\frac{j\pi V_m \sin \omega_m t}{V_\pi}} \right] + \right. \\
&+ \left. \left[ e^{\frac{j\pi V_m \sin(\omega_m t + \pi/2)}{V_\pi}} + e^{-\frac{j\pi V_m \sin(\omega_m t + \pi/2)}{V_\pi}} \right] \right\} \\
&= E_0 e^{j\omega_c t} \sum_{n=-\infty}^{\infty} J_{4n}(m) e^{j4n\omega_m t}
\end{aligned} \quad (1)$$

where  $m = \pi V_{pp} / (2V_\pi) = \pi V_m / V_\pi$  is modulation index (MI), and  $V_{pp} = 2V_m$  is the peak-to-peak voltage of the RF local oscillator signal.  $V_\pi$  is the half-wave voltage of sub-MZMs. The optical carrier becomes zero ( $J_0(m)=0$ ) when the modulation index is  $m = 2.4048$ , and the output of the first DP-MZM could be approximated to:

$$\begin{aligned}
E_1(t) &\approx E_0 e^{j\omega_c t} [J_4(m)(e^{j4\omega_m t} + e^{-j4\omega_m t}) + \\
&+ J_8(m)(e^{j8\omega_m t} + e^{-j8\omega_m t})]
\end{aligned} \quad (2)$$

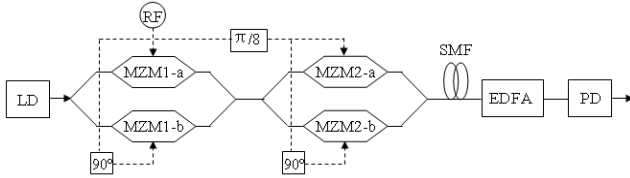


Fig. 1. Schematic diagram of optical mm-wave generation based on frequency 16-tupling. LD: Laser diode; MZM: Mach-Zehnder Modulator; RF: Radio frequency; SMF: Single mode fiber; EDFA: Er-doped fiber amplifier; PD: Photo diode

Notably, optical frequency octupling is obtained after first DP-MZM. The generated optical mm-wave signal from the first DP-MZM is then send into the second DP-MZM. Both of the sub-MZMs (MZM2-a and MZM2-b) are biased at the full point. Note that a  $\pi/8$  phase shift is introduced between the driving signals of the first and second DP-MZMs. Therefore, the optical field at the output of the second DP-MZM can be expressed as:

$$\begin{aligned}
E_2(t) &= E_0 e^{j\omega_c t} [J_4(m)(e^{j4\omega_m t} + e^{-j4\omega_m t}) + \\
&+ J_8(m)(e^{j8\omega_m t} + e^{-j8\omega_m t})] \times \left\{ J_4(m) \left[ e^{j4(\omega_m t + \frac{\pi}{8})} + e^{-j4(\omega_m t + \frac{\pi}{8})} \right] + \right. \\
&+ J_8(m) \left[ e^{j8(\omega_m t + \frac{\pi}{8})} + e^{-j8(\omega_m t + \frac{\pi}{8})} \right] \left. \right\} = E_0 e^{j\omega_c t} \left\{ J_4^2(m) \left[ e^{j(8\omega_m t + \pi/2)} + \right. \right. \\
&+ e^{-j(8\omega_m t + \pi/2)} \left. \right] + J_4(m) J_8(m) \left[ e^{j(4\omega_m t + \frac{\pi}{2})} + e^{-j(4\omega_m t + \frac{\pi}{2})} \right. \\
&+ e^{j(4\omega_m t - \frac{\pi}{2})} + e^{-j(4\omega_m t - \frac{\pi}{2})} \left. \right] + e^{j(12\omega_m t + \pi)} + e^{-j(12\omega_m t + \pi)} + e^{j(12\omega_m t + \frac{\pi}{2})} \\
&+ e^{-j(12\omega_m t + \frac{\pi}{2})} \left. \right\}
\end{aligned} \quad (3)$$

According to the characteristics of the Bessel functions ( $J_8(2.4048) \ll J_4(2.4048)$ ), it can be found from Eq.(3) that only eighth-order sidebands are obtained at the output of the second DP-MZM. After square-law detection using a photo diode (PD), the electrical signal with frequency sixteen times that of the RF driven signal is obtained.

## 2.2. Imperfect EXT of Each Sub-MZM

The MZM extinction ratio (EXT) is an important factor in carrier suppressed optical mm-wave signal generation schemes. The theoretical deduction above is based on the assumption that each sub-MZM has a perfect EXT. However, the EXTs of commercially available MZMs are finite due to amplitude imbalance in MZM arms, and the optical carrier is not totally suppressed with imperfect EXT. Under non-ideal condition with finite sub-MZM EXT, the optical field at the output of the second DP-MZM can be expressed as:

$$\begin{aligned}
E_2(t) &= \frac{E_0}{4} e^{j\omega_c t} \left\{ \left[ e^{j m \sin \omega_m t} + \gamma e^{-j m \sin \omega_m t} \right] + \right. \\
&+ \left. \left[ e^{j m \sin(\omega_m t + \theta)} + \gamma e^{-j m \sin(\omega_m t + \theta)} \right] \right\} \cdot \\
&\cdot \left\{ \left[ e^{j m \sin(\omega_m t + \Delta\phi)} + \gamma e^{-j m \sin(\omega_m t + \Delta\phi)} \right] + \right. \\
&+ \left. \left[ e^{j m \sin(\omega_m t + \theta + \Delta\phi)} + \gamma e^{-j m \sin(\omega_m t + \theta + \Delta\phi)} \right] \right\} \\
&= \frac{E_0}{4} e^{j\omega_c t} \sum_{n=-\infty}^{+\infty} A_n e^{jn\omega_m t}
\end{aligned} \quad (4)$$

And there is

$$A_n = \left\{ \begin{aligned} & \left\{ [(1+\gamma^2)J_n(a) + 2\gamma J_n(b)] [e^{jn\Delta\phi/2} (1+e^{jn\theta})] + \right. \\ & + [(1+\gamma^2)[J_n(c) + J_n(d)] + 2\gamma[J_n(e) + J_n(f)] \left. \right\} e^{jn(\Delta\phi+\theta)/2}, n=4k \\ & \left\{ [(1+\gamma^2)J_n(a) - 2\gamma J_n(b)] [e^{jn\Delta\phi/2} (1+e^{jn\theta})] + \right. \\ & + [(1+\gamma^2)[J_n(c) + J_n(d)] - 2\gamma[J_n(e) + J_n(f)] \left. \right\} e^{jn(\Delta\phi+\theta)/2}, n=4k+2 \\ & \left\{ [(1-\gamma^2)J_n(a) e^{jn\Delta\phi/2} (1+e^{jn\theta})] + \right. \\ & + \left. \left. [(1-\gamma^2)[J_n(c) + J_n(d)] e^{jn(\Delta\phi+\theta)/2}] \right\}, n=4k+1 \text{ or } 4k+3 \end{aligned} \right. \quad (5)$$

where  $\gamma$  is a scaling factor between 0 and 1 that accounts for a non-ideal device, and the parameter is related to the EXT of each sub-MZM  $\varepsilon$  by  $\gamma = (\sqrt{\varepsilon} - 1) / (\sqrt{\varepsilon} + 1)$ , and

$$\begin{aligned}
a &= 2m \cos(\Delta\phi/2), \quad c = 2m \cos[(\theta + \Delta\phi)/2], \quad e = 2m \sin[(\theta + \Delta\phi)/2] \\
b &= 2m \sin(\Delta\phi/2), \quad d = 2m \cos[(\theta - \Delta\phi)/2], \quad f = 2m \sin[(\theta - \Delta\phi)/2]
\end{aligned} \quad (6)$$

Note that the optical power of each optical sideband

$P_n$  could be easily deduced from Eq. (5) and (6).

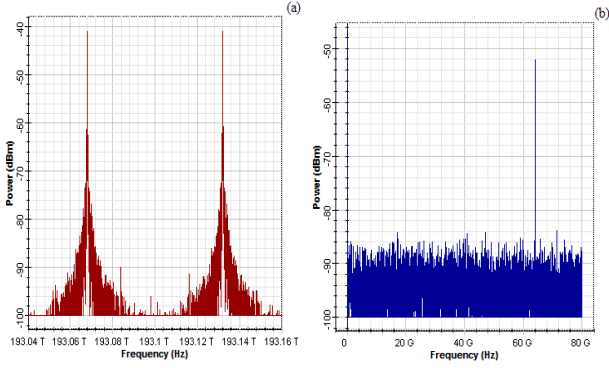


Fig. 2. (a) Optical spectrum, (b) RF spectrum of generated 64 GHz optical mm-wave with 4 GHz microwave drive signal

### 3. Results and discussion

In order to access the validity of the proposed 16-tupling mm-wave generation scheme shown in Fig. 1, a simulation is carried out using the commercial software package OptiSystem with the simulation parameters following the theoretical values. The output optical carrier frequency of LD and driven signal frequency applied to sub-MZM is 193.1 THz and 4 GHz, respectively.

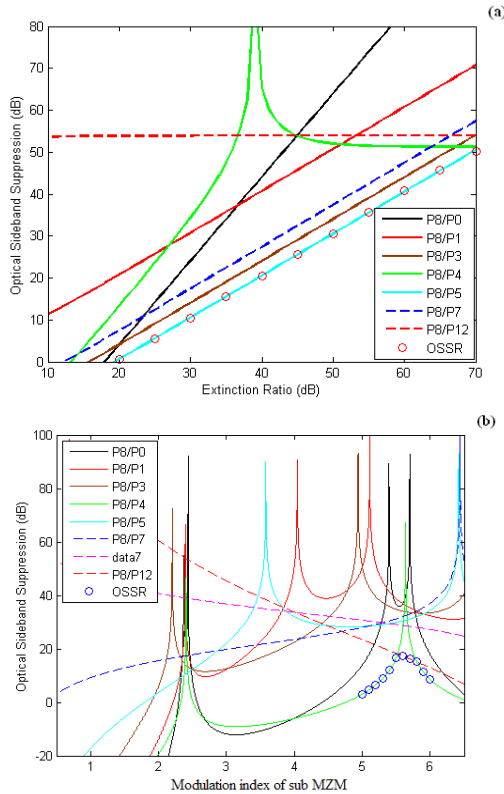


Fig. 3. Theoretical optical sideband suppression (lines) and simulated OSSR (circle) against (a) non-ideal EXT  $\epsilon$  ( $m = 2.4048$ ) and (b) MI  $m$  ( $\epsilon = 30$  dB) in the frequency 16-tupling scheme

Fig. 2(a) and Fig. 2(b) shows the optical spectra, RF spectra of the generated optical mm-wave with modulation index (MI) of sub-MZM at  $m = 2.4048$ , respectively. It can be seen clearly that the proposed scheme can generate an optical mm-wave consisting of two main tones with a frequency spacing of 64 GHz, which is 16 times of driven signal frequency. The undesired optical sidebands are well suppressed, so the RF spectrum mainly consists of dc and the 64 GHz harmonic. Note that the EXT of MZM is assumed to be 100 dB.

The theoretical and simulated OSSR evolution of the frequency 16-tupling scheme that considers EXT and MZM modulation index (MI) is investigated in Fig. 3. As can be seen from Fig. 3(a), the OSSR increases with the increasing of EXT. MI is assumed to be 2.4048. Fig. 3 (b) indicates that exist an optimal MI, the maximal OSSR 18.2 dB is obtained in which  $m = 5.52$  and EXT is assumed to be 30 dB. Using MZM with low half-wave voltage can lead to a high MI [13]. The OSSR is higher than 15 dB, which is sufficient for most mm-wave applications [14, 15]. The simulation results agree well with the theoretical results.

The OSSR as a function of EXT with and without MZM MI optimizing is shown in Fig. 4. We can see clearly that the system performance is improved by optimizing MI when the EXT is no more than 40 dB. For example, with a typical EXT of 30 dB, OSSR increased from 10.5 dB to 18.2 dB. The simulation results agree well with the theoretical results.

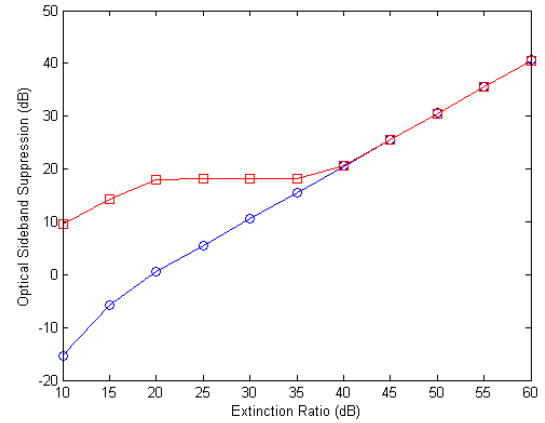


Fig. 4. OSSR against EXT with (red) and without (blue) MI optimizing. Theoretical (lines), Simulated OSSR (square and circle)

To evaluate the performance of the proposed scheme, optical sideband suppression ratio (OSSR) degradation with MZM bias drift is also investigated. Fig. 5(a) depicts the OSSR degradation with bias drift of one sub-MZM (MZM1-a). The OSSR degrades from 49 dB to 10.2 dB with 5% bias drift ratio. The bias drift ratio is defined as  $(\Delta V/V_m) \times 100\%$ , where  $\Delta V$  is bias voltage deviation. Fig. 5(b) shows the OSSR degradation with bias drift of two sub-MZMs. As can be seen from Fig. 5, to suppress undesired optical sidebands effectively and obtain high

quality mm-wave signals, the bias drift of MZM need to be controlled. For example, to maintain 15 dB OSSR, bias drift ratios of two sub-MZMs should be controlled within  $\pm 2\%$  of half-wave voltages.

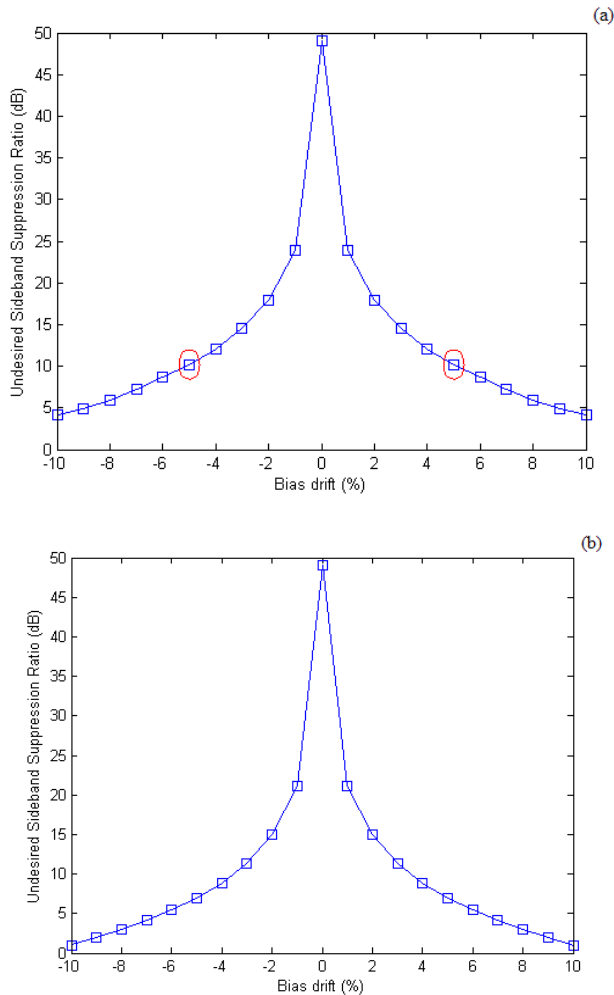


Fig. 5. OSSR versus (a) one sub-MZMs bias drift ratio and (b) two sub-MZMs bias drift ratio

To analyze the influence of non-ideal phase shift on the quality of the generated optical mm-wave, OSSR and RF spurious suppression ratio (RSSR) degradation with phase drift of the phase shifter between MZM1 and MZM2 are evaluated. The OSSR and RSSR versus the phase drift is shown in Fig. 6(a) and Fig. 6(b), respectively. It can be seen clearly that the phase drift should be less than  $\pm 5\%$  to maintain 15 dB OSSR and 10 dB RSSR.

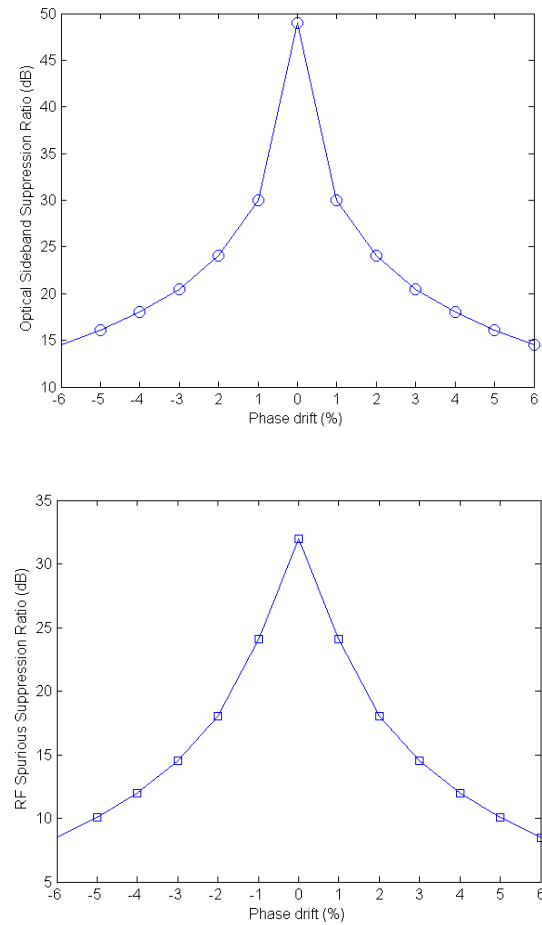


Fig. 6. OSSR (a) and RSSR (b) versus phase drift of phase shifter between MZM1 and MZM2

#### 4. Conclusion

A novel frequency 16-tupling scheme based on two cascaded integrated DP-MZMs is proposed for the high frequency optical mm-wave generation without optical filtering, the impact of EXT and MI on performance evolutions of the scheme is investigated. The theoretical analysis and simulation verification are both presented. The results show that an optical mm-wave generation with frequency 16-tupling of the local oscillator can be generated by properly adjusting local oscillator voltage and phase shift between the driving signals of the first and second DP-MZMs. The frequency 16-tupling system is susceptible to the influence of non-ideal EXT of MZM. The OSSR could be improved by MI optimizing. For example, with a typical EXT of 30 dB, the OSSR increased from 10.5 dB to 18.2 dB. In addition, the OSSR is higher than 15 dB when the bias drift ratios of two sub-MZMs are controlled within  $\pm 2\%$  of half-wave voltages. Moreover, the phase drift of phase shifter between MZM1 and MZM2 should be limited within  $\pm 5\%$  to maintain 15 dB OSSR and 10 dB RSSR.

### Acknowledgements

This work was supported in part by the Science Foundation of Hubei Province (Grant No. 2012FFB03702) and the Science Foundation of Hubei Education Committee (Grant No. D20141203).

### References

- [1] J. Yao, *Journal of Lightwave Technol.* **27**(3), 314 (2009).
- [2] A. J. Seeds, K. J. Williams, *Journal of Lightwave Technol.* **24**(12), 4628 (2006).
- [3] Q. Sun, J. Wang, J. Wo, X. Li, D. Liu, *Microw. Optical Technol. Lett.* **53**(11), 2478 (2011).
- [4] Z. Zhu, S. Zhao, Q. Tan, D. Liang, X. Li, K. Qu, *IEEE Trans. Microw. Theory Tech.* **64**(11), 3748 (2016).
- [5] Z. Zhu, S. Zhao, Y. Li, X. Chu, X. Wang, G. Zhao, *IEEE Journal of Quantum Electronics* **49**(11), 919 (2013).
- [6] Z. Zhu, S. Zhao, Y. Li, X. Chen, X. Li, *Optics & Laser Technology* **65**, 29 (2015).
- [7] W. Li, J. Yao, *IEEE Photon. Technol. Lett.* **22**(1), 24 (2010).
- [8] Z. Zhu, S. Zhao, W. Zheng, W. Wang, B. Lin, *Applied Optics* **54**(32), 9432 (2015).
- [9] Z. Zhu, S. Zhao, X. Chu, Y. Dong, *Optics Communications* **354**, 40 (2015).
- [10] X. Li, S. Zhao, Z. Zhu, B. Gong, X. Chu, Y. Li, *Journal of Modern Optics* **62**(18), 1502 (2015).
- [11] J. Ma, X. Xin, J. Yu, C. Yu, K. Wang, H. Huang, L. Rao, *Journal of Optical Network.* **7**(10), 837 (2008).
- [12] X. Chen, L. Xia, D. Huang, *Journal of Optical Communications* **37**(3), 295 (2016).
- [13] J. Kondo, K. Aoki, Y. Iwata, A. Hamajima, T. Ejiri, O. Mitomi, M. Minakata, *International Top Meeting on Microwave Photonics*, 1-4 (2005).
- [14] C. T. Lin, J. Chen, S. P. Dai, P. C. Peng, S. Chi, *IEEE J. Lightwave Technol.* **26**(15), 2449 (2008).
- [15] H. Kiuchi, T. Kawanishi, M. Yamada, T. Sakamoto, M. Tsuchiya, J. Amagai, M. Izutsu, *IEEE Trans. Microw. Theory Tech.* **55**(9), 1964 (2007).

---

\*Corresponding author: xgchen826@yahoo.com